

# 基于飞秒激光的 Pt-TiO<sub>2</sub> 纳米连接及其电学性能调控

邢松龄, 肖宇, 霍金鹏, 林路禅, 沈道智, 刘磊\*

清华大学机械工程系, 北京 100084

**摘要** 研究了金属-氧化物异质材料纳米连接过程中的飞秒激光能量输入特征, 实现了纳米材料快速低损伤互连的同时, 保证了器件功能的完整性。研究了纳米连接对 Pt-TiO<sub>2</sub> 跨尺度互连结构电学性能调控的影响。实验结果表明: 当入射光能量密度为 5.02 mJ/cm<sup>2</sup> 时, 纳米线与电极接触区域形成具有稳定结合强度的互连接头。模拟结果显示, 飞秒激光辐照一侧产生局部“热点”, 增强了接头区域的光学吸收。互连接头的形成, 降低了异质界面的接触势垒。同时, 基于互连结构模拟神经元突触传递, 实现了更加稳定的电学性能调控。

**关键词** 激光技术; 纳米连接; 飞秒激光; 忆阻器; 突触可塑性; 二氧化钛纳米线

中图分类号 O439 文献标志码 A

doi: 10.3788/CJL202148.0802004

## 1 引言

随着纳米材料尺度的不断减小, 材料的成形和制造也遇到了诸多瓶颈, 单一结构的纳米材料很难满足越来越复杂的功能需求<sup>[1-2]</sup>, 因此, 对未来纳米制造领域提出了多材料、跨尺度、多功能等需求。作为一种自下而上的纳米材料加工成形方法, 纳米尺度的材料连接(以下简称“纳米连接”)不仅可以实现纳米尺度下异质材料的选择性组合, 同时在提高互连材料力学性能的基础上, 可以对不同材料的性能进行结合, 实现具有复杂功能器件的成形, 并保证其功能的稳定输出<sup>[3-4]</sup>。因此, 纳米连接已成为先进微纳器件制造和微纳系统封装集成的关键环节。

二氧化钛(TiO<sub>2</sub>)作为典型的宽禁带氧化物半导体, 被广泛应用于电学器件<sup>[5]</sup>、光触媒催化<sup>[6]</sup>等领域。然而, 热平衡状态下 TiO<sub>2</sub> 和部分金属材料不润湿, 如铂(Pt)、金(Au), 难以发生原子层相互扩散的界面行为, 从而限制了异质结的电荷传输能力, 影响了器件的进一步应用。近年来, 关于光辐照激发金属-介电表面等离激元用于纳米材料连接的研究不断深入。以飞秒激光为代表的超短脉冲激光, 其单脉冲携带能量较大, 且与材料作用过程中产生的

热量积累较小, 有利于纳米材料的加工成形<sup>[7-9]</sup>, 特别是金属-高熔点氧化物的互连。

本文基于二维金属 Pt 电极-TiO<sub>2</sub> 纳米线结构, 研究了飞秒激光辐照下金属-半导体异质结构的跨尺度互连。利用飞秒激光辐照下激发的表面等离激元效应, 实现了异质界面处能量的可控输入。基于纳米连接实现异质材料间的界面修饰, 构建具有模拟神经元突触传递功能的器件单元, 探究选区界面修饰对器件性能调控的影响。

## 2 材料与方法

采用水热法制备 TiO<sub>2</sub> 纳米线<sup>[10]</sup>。在 900 ℃下保温 2 h, 获得具有金红石相的 TiO<sub>2</sub> 纳米线。采用单面抛光的单晶硅片作为基板, 经氧化、光刻、显影、磁控溅射等一系列半导体工艺流程, 在硅片表面沉积约 200 nm 厚的 Pt 电极。将 TiO<sub>2</sub> 纳米线分散在去离子水中, 而后使用移液枪吸取少量纳米线溶液并滴落在带电极的硅片上, 并在空气中自然干燥。

实验用飞秒激光器为美国相干公司 4 W 钛宝石飞秒激光系统, 其脉冲宽度为 50 fs, 重复频率 0~1 kHz 可调, 波长为 800 nm。激光光束首先通过开闭时间可控的机械快门, 经一系列中性衰减片、半波

收稿日期: 2020-11-30; 修回日期: 2021-01-03; 录用日期: 2021-01-11

基金项目: 国家重点研发计划(2017YFB1104900)、国家自然科学基金(51775299, 52075287, 51520105007)

\*E-mail: liulei@tsinghua.edu.cn

片、偏振片、反射镜被导入至光学显微镜中,而后经一定数值孔径(NA)的物镜光阑聚焦至样品表面,并配合电动位移平台进行样品移动,光路如图1所示。

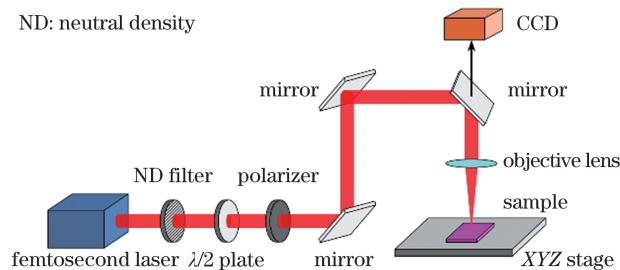


图1 飞秒激光纳米连接示意图

Fig. 1 Schematic of femtosecond laser-induced nanowelding

使用多物理场软件(COMSOL Multiphysics v5.2)并基于有限元原理,对纳米尺度下Pt-TiO<sub>2</sub>结构的空间电场分布进行仿真。使用扫描电子显微镜(Zeiss Gemini)对纳米结构微观形貌进行观测,使用原子力显微镜(Bruker Dimension)对纳米焊点强度进行定性表征,使用高精度源表(Agilent B2901A)对焊后的电极-纳米线结构进行电学表征。

### 3 结果与讨论

#### 3.1 飞秒激光辐照TiO<sub>2</sub>纳米线和Pt电极互连

二维金属电极和一维纳米线本质上是跨尺度结构,考虑到金属与半导体材料在力学、光学、热学性质上的巨大差异,飞秒激光辐照下的材料行为将受到材料属性和几何结构的影响。如图2所示,使用物镜( $NA=0.5$ )聚焦后的飞秒激光对Pt基板上的TiO<sub>2</sub>纳米线进行一定间隔的辐照(光斑位于圆点处),可获得具有独立烧蚀特征的损伤结构。对比整体辐照下的材料行为<sup>[11]</sup>,局域辐照下的能量分布更加集中,光-热转换效率更高,从而实现空间高能量的精准定位输入。

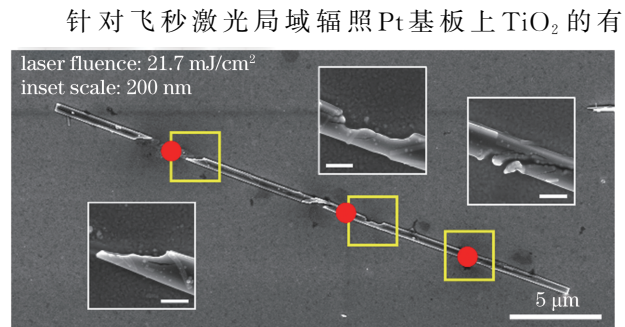


图2 飞秒激光局域辐照TiO<sub>2</sub>纳米线的损伤效果

Fig. 2 Damages of single TiO<sub>2</sub> nanowire under femtosecond laser localized irradiation

限损伤特性,通过调整入射光参数,可以实现金属电极与半导体纳米线的互连。如图3所示,当入射光能量密度为5.02 mJ/cm<sup>2</sup>时,纳米线与电极接头区域发生熔融。当纳米线直径小于200 nm时,端部的熔化现象更加明显,并且表现出了部分烧蚀特征,在烧蚀较强的位置,由于库仑爆炸的作用,材料被抛离出纳米线基体,形成的纳米颗粒附着在熔化区周围。当纳米线直径达到500 nm时,端部仅发生局部熔化,形成类似于点焊的互连结构。与此同时,在纳米线基体与基板悬空处并未出现形貌损伤,表明飞秒激光的局域辐照实现了能量的有限输入,并且保证了材料损伤的最小化。

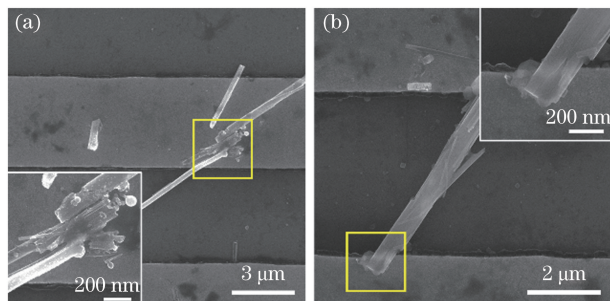


图3 Pt-TiO<sub>2</sub>互连接头形貌。(a) 纳米线直径为

200 nm;(b) 纳米线直径为500 nm

Fig. 3 Morphology of Pt-TiO<sub>2</sub> bondings. (a) Diameter of TiO<sub>2</sub> nanowires is 200 nm; (b) diameter of TiO<sub>2</sub> nanowires is 500 nm

互连的Pt-TiO<sub>2</sub>结构存在一定的结合强度,在原子力显微镜探针作用下表现出不同的力学反馈。如图4所示,能量密度为5.02 mJ/cm<sup>2</sup>的入射光辐照纳米线点1区域,形成单侧互连结构。在原子力显微镜接触模式下,探针从左至右依次划过点1及未经辐照的点2区域,获得不同的力学反馈结果。结果显示,互连接头1处的加载和卸载的力学曲线重合,表明此处具有良好的界面连接。点2处的加载和卸载曲线产生较大分离,表明此处存在塑性形变,对应纳米线和电极的无互连接头在原子力探针的接触作用下发生微小位移。从而可以得知,在特定激光能量密度辐照下,互连接头的界面结合强度得到了提升。

单晶TiO<sub>2</sub>结构稳定,且在宏观状态下能和Pt原子形成有效的结合,因此热平衡条件下Pt与TiO<sub>2</sub>的润湿性极差。然而,飞秒激光辐照单晶TiO<sub>2</sub>的稳定结构时,会对晶体结构特别是Ti—O键造成破坏,从而使材料表面发生相变行为,生成非化学计量比的金属钛的氧化物Magnéli相( $TiO_{2-x}$ )<sup>[12-13]</sup>。此

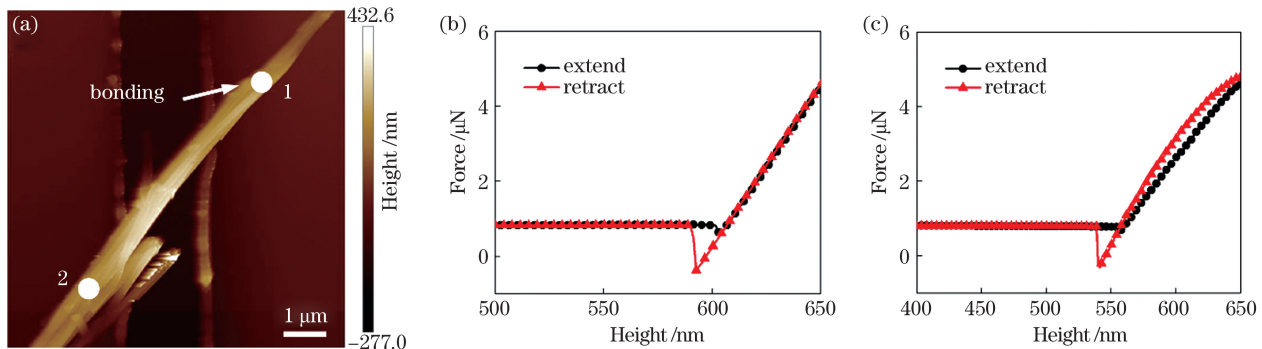


图 4 Pt-TiO<sub>2</sub> 互连接头强度表征。(a)接头的原子力显微形貌;(b)点1的加载/卸载力学反馈;(c)点2的加载/卸载力学反馈  
Fig. 4 Strength characterization of Pt-TiO<sub>2</sub> bonding. (a) Atomic force microscopic morphology of bonding; (b) curves of the extend/retract force at point 1; (c) curves of the extend/retract force at point 2

时,存在多余悬挂键的Ti原子将增加与Pt的亲和作用,改变氧化物稳定的氧结合作用,进而获得异质界面修饰的互连接头,提高了TiO<sub>2</sub>纳米线和金属电极的结合强度。针对此类尺度较小的互连接头,常规的电子束能谱穿透力较强,不能很好反映材料表面的化学成分,可采用纳米俄歇能谱对接头熔化区表面几个纳米的原子层进行表征<sup>[14]</sup>。得益于纳米线自身结构的变化,在电极表面的TiO<sub>2</sub>可与Pt形成一定的润湿铺展,如图5所示。

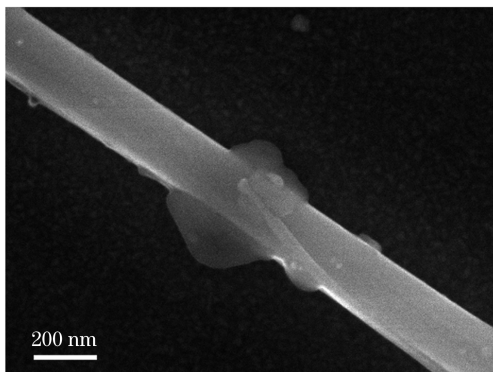


图 5 Pt-TiO<sub>2</sub> 互连接头浸润性表征

Fig. 5 Characterization of infiltration at Pt-TiO<sub>2</sub> bonding

### 3.2 飞秒激光辐照下的局域电场分布

光辐照金属-介电结构会激发界面处的表面等离激元效应,并且局域“热点”在无限大的平界面中呈周期性分布<sup>[15]</sup>。对于Pt-TiO<sub>2</sub>结构,此时金属材料的尺度远大于半导体介电材料,表面等离激元的分布将受到材料尺度的限制从而在空间受到约束,并影响纳米线结构的能量输入状态。图6为搭建的Pt-TiO<sub>2</sub>结构模型,包括电极-纳米线的接头区域和中间悬空部分的空气-纳米线环境。根据实验中的纳米线直径范围,设定模拟过程中的纳米线直径为200 nm,电极高度为250 nm,入射高斯光束直径为

1 μm,并且不考虑激光与材料相互作用对几何结构产生的变形影响。模拟结果显示,稳态下电场在两侧电极呈非对称分布。光辐照一侧Pt-TiO<sub>2</sub>接头处是“热点”集中区域,而远离辐照一侧电极-纳米线接头部位和悬空结构有较低的电场增强效应。由结构中的电场分布特征可知,飞秒激光局域辐照能够在空间中实现入射能量的选择性输入,并将电场增强局限在辐照一侧的接头部位,从而实现局域辐照下纳米线材料的低损伤互连。

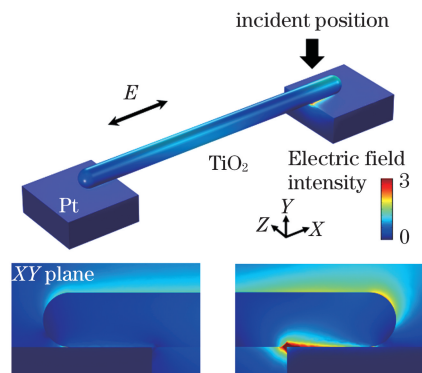


图 6 Pt-TiO<sub>2</sub> 结构在局域光辐照下的电场分布

Fig. 6 Electric field distribution of Pt-TiO<sub>2</sub> bonding under localized irradiation

### 3.3 Pt-TiO<sub>2</sub> 异质界面结构的调控

由于Pt和TiO<sub>2</sub>费米能级的差异,热平衡条件下二者接触时,界面处将形成具有较高势垒的肖特基接触。而飞秒激光辐照下形成的Pt-TiO<sub>2</sub>连接结构处存在复合界面,部分还原的Magnéli相除了对金属与半导体的连接起到促进作用,其内部存在的大量氧空位缺陷还可以大大降低异质结的界面势垒,使界面在偏压作用下具有更好的电学传导特性<sup>[14]</sup>。此外,连接接头的形成还能增强原子间的结合,消除机械结合形成的范德瓦尔斯力接触带来的

接触电势差,进一步促进界面处接触势垒的降低,增强了界面处的电学传导。如图7所示,使用飞秒激光对Pt-TiO<sub>2</sub>-Pt搭接结构的一侧进行连接,另一侧保持自然搭接状态,获得具有整流特征的电学传输信号。

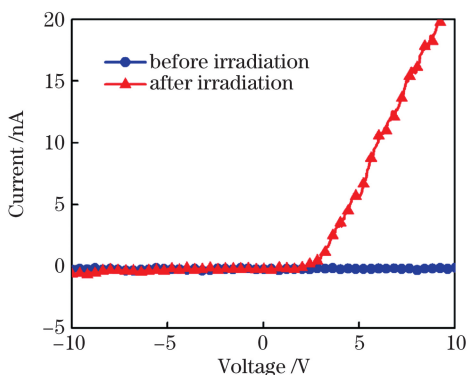


图7 飞秒激光单端互连前后 Pt-TiO<sub>2</sub> 结构的电流响应

Fig. 7 Current response of Pt-TiO<sub>2</sub> nanowire before and after one-side welding by femtosecond laser

对自然状态下的TiO<sub>2</sub>纳米线两端施加偏压,也可在近负极一侧界面处获得部分还原的Magnéli相,但此时Magnéli相的形成并非由于与外界发生氧化还原反应,而是因为在偏压作用下缺陷在材料内部的移动<sup>[16]</sup>。若施加的初始偏压较小,在交变电场的作用下,缺陷在纳米线内部会发生二次迁移。若施加的初始偏压较大,虽然产生的缺陷不随后续电压的循环而消除,但是缺陷的偏聚使TiO<sub>2</sub>纳米线其他部分的缺陷密度降低,提升了纳米线整体的电阻率。因此,往往需要长时电压循环来使其内部的Magnéli相分布稳定,且稳定后电流水平与初始状态相比较低。飞秒激光纳米连接对异质界面的修饰,可以在局部直接产生大量的稳定Magnéli相,从而免去初始化环节。

### 3.4 基于Pt-TiO<sub>2</sub>互连结构模拟神经元突触电信号传输

图8(a)显示生物突触结构接收刺激时化学物质在神经元间传递的示意图。神经元之间的信息传递包括三个步骤:电信号传导至轴突末端,激活钙离子通道并转换为化学信号,而后释放神经递质;神经递质经扩散通过突触间隙;神经递质与树突的受体结合,引发进一步的化学反应,最终改变后一神经元的膜电位,产生树突电流<sup>[17-18]</sup>。

图8(b)为在单个纳米线结构中模拟突触间信号传递的示意图,由两个间距为3 μm的Pt电极桥接单根TiO<sub>2</sub>纳米线组成。在外部电脉冲刺激下,

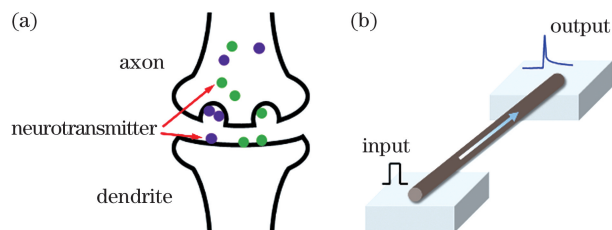


图8 单纳米线用于突触信号传递研究示意图。(a)突触模型;(b)脉冲刺激下的单纳米线

Fig. 8 Schematic of the nanowire for the synaptic response study. (a) Synapse model; (b) single TiO<sub>2</sub> nanowire under pulse excitation

左侧电极(突触前神经元)中的电位通过纳米线(突触)传递到右侧电极(突触后神经元),同时产生电流响应并随时间逐步衰减(兴奋性突触后电流)。为了在纳米线中模拟兴奋性神经递质刺激突触下的反应,将一系列幅值为10~20 V、持续时间为100 ms的脉冲电压施加到输入端Pt电极上,并在脉冲之间保持足够长的时间间隔,获得如图9所示的输出端电流响应。随着输入端电压脉冲的幅值从10 V增加到20 V,输出端的电流峰值从27.2 nA增加到72.5 nA,如图9所示。

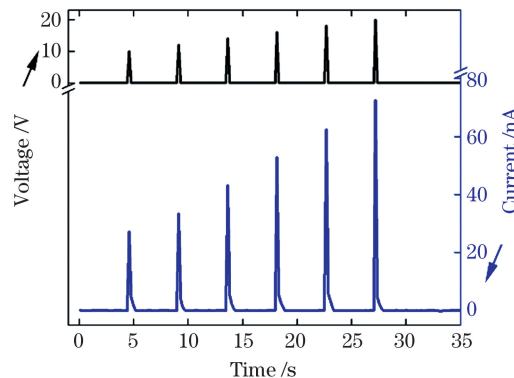


图9 TiO<sub>2</sub> 纳米线在分离单脉冲刺激下的电流响应

Fig. 9 Current response of Pt-TiO<sub>2</sub> nanowire under divided monopulse excitation

前述结果表明,飞秒激光辐照电极-纳米线产生互连结构,同时会在异质界面处预置缺陷层。结构与界面状态的修饰,保证了电极-纳米线结构在电脉冲激励下的功能稳定。使用上述单脉冲电压组合对单侧局部修饰的TiO<sub>2</sub>纳米线进行连续多次激励,通过延长脉冲之间的间隔(比脉冲持续时间长得多),保证纳米线充足的自然弛豫时间。如图10(a)所示,激光修饰后的纳米线结构具有高度可重复性和可控的多级电流响应,并且实验中持续多达10<sup>3</sup>次循环。而对于未经激光处理直接构造的电极-纳米线结构,直接施加电脉冲刺激后将得到漫长的初

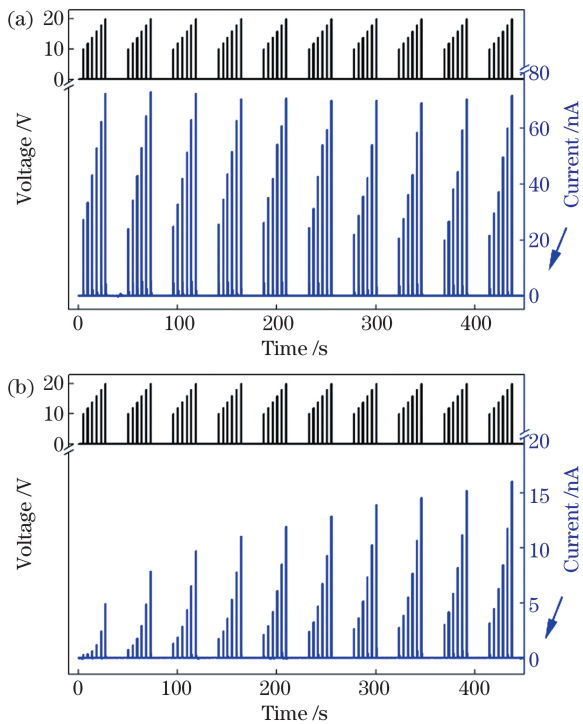


图 10  $\text{TiO}_2$  纳米线在组合单脉冲刺激下的电流响应。

(a) 焊接后; (b) 未焊接

Fig. 10 Current response of a  $\text{TiO}_2$  nanowire under excitation of a series of pulses. (a) After welding; (b) before welding

始化过程,如图 10(b)所示,在进行 10 次电脉冲循环后,其响应电流峰值仍保持增加的趋势。在该过程中,由于初始状态下阳极处的氧空位缺陷较少,需

较高的预置电压来获得修饰的界面层,随着电脉冲的不断刺激,材料内部缺陷结构不断积累,造成了不稳定的电流响应特征。从而在  $\text{TiO}_2$  纳米线模拟神经元突触的结构中,飞秒激光的互连与界面修饰能够保证结构在连续电脉冲刺激下的稳定性并实现更加复杂的功能。

基于 Pt-TiO<sub>2</sub> 互连结构,通过施加多个持续时间为 300 ms、电压峰值为 10 V 的电脉冲激励来模拟学习过程,并通过随后的电流持续衰减特性模拟遗忘过程。模拟遗忘过程的读取电压为 +2 V。经过 100 个电脉冲刺激后,纳米线中所得的电流增强和衰减曲线如图 11(a)、(b) 所示,回路中的电流随时间增加呈近似指数衰减的特征。电流的自发衰减类似于人脑中的记忆丧失或遗忘曲线,通过重复刺激,可以在单个纳米线结构中从短期增强转变为长期增强。如图 11(c) 所示,随着电脉冲刺激的数量( $N$ )增加,100 s 时衰减电流的归一化百分比从 1.4%(脉冲数为 5)提高到 33.1%(脉冲数为 400)。电流衰减的时间常数也随着脉冲数的增加而增大,如图 11(d) 所示,并且经过大约 600 次脉冲刺激后达到饱和。此外,遗忘速率的减慢表明,飞秒激光局域修饰的  $\text{TiO}_2$  纳米线结构在重复刺激下,激励电流的幅值及持续时间明显提升。该结果表明,多脉冲电激励下的稳定电学响应很好地模拟了神经系统中由于膜电位的频繁刺激而产生的突触强度增加效果。

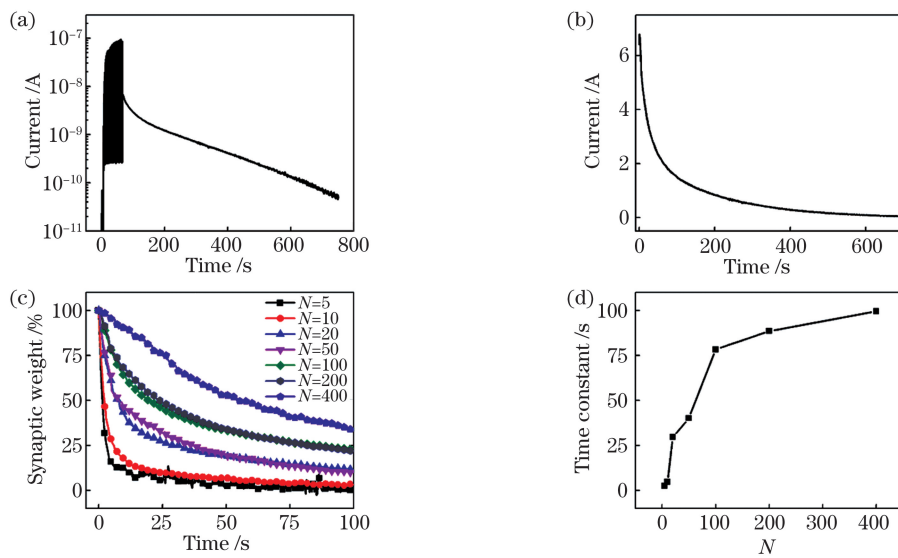


图 11 Pt-TiO<sub>2</sub> 互连结构模拟突触的长时记忆特征。(a) 电脉冲数  $N=100$  时的记忆和遗忘特征; (b) 电脉冲数  $N=100$  时的电流衰减曲线; (c) 不同脉冲数刺激下的归一化电流衰减曲线; (d) 不同脉冲数刺激下的电流衰减时间常数

Fig. 11 Characteristics of long-term memory of synapse simulated by the Pt-TiO<sub>2</sub> bonding. (a) Learning and forgetting curve with the number of electric pulses  $N=100$ ; (b) current decay curve with the number of electric pulses  $N=100$ ; (c) normalized current attenuation curve under different pulse number stimulation; (d) current decay time constant under different pulse number stimulation

## 4 结 论

使用飞秒激光实现了金属 Pt 和半导体氧化物  $TiO_2$  纳米线的跨尺度连接。调节激光入射功率可以改变纳米线的损伤程度,在  $5.02\text{ mJ/cm}^2$  能量密度下获得具有良好结合强度的 Pt-TiO<sub>2</sub> 异质接头。聚焦的飞秒激光辐照使 Pt-TiO<sub>2</sub> 在界面处获得受限的表面等离激元增强效应,未辐照区域则获得相对低的能量输入,保证互连接头的低损伤。飞秒激光辐照下的有限热输入使 TiO<sub>2</sub> 纳米线发生相变,获得的缺陷态结构具有改善的润湿特性,降低了纳米线与金属电极的接触势垒。接头的互连提高了器件电学传输的稳定性,具体表现为在 TiO<sub>2</sub> 纳米线模拟神经元突触的结构中,不需要较高的偏置电压来获得修饰的界面层,简化了器件的初始化过程。同时,在连续电脉冲刺激下,纳米线互连结构表现出较高的稳定性并实现更加复杂的长时记忆功能。

**致谢** 本研究得到清华大学机械工程系邹贵生教授的大力支持和指导。

## 参 考 文 献

- [1] Waldrop M M. The chips are down for Moore's law [J]. Nature, 2016, 530(7589): 144-147.
- [2] Huo J P, Zou G S, Lin L C, et al. Highly focused femtosecond laser directed selective boron doping in single SiC nanowire device for n-p conversion [J]. Applied Physics Letters, 2019, 115(13): 133104.
- [3] Chen C X, Lu Y, Kong E S, et al. Nanowelded carbon-nanotube-based solar microcells [J]. Small (Weinheim an Der Bergstrasse, Germany), 2008, 4(9): 1313-1318.
- [4] Lee C, Oh Y, Yoon I S, et al. Flash-induced nanowelding of silver nanowire networks for transparent stretchable electrochromic devices [J]. Scientific Reports, 2018, 8(1): 2763.
- [5] Zhang D, Liu W W, Tang L, et al. High performance capacitors via aligned TiO<sub>2</sub> nanowire array [J]. Applied Physics Letters, 2017, 110(13): 133902.
- [6] Cai J M, Wang Y T, Zhu Y M, et al. *In situ* formation of disorder-engineered TiO<sub>2</sub> (B)-anatase heterophase junction for enhanced photocatalytic hydrogen evolution [J]. ACS Applied Materials & Interfaces, 2015, 7(45): 24987-24992.
- [7] Wu X F, Yin H L, Li Q. Femtosecond laser processing of carbon nanotubes film [J]. Chinese Journal of Lasers, 2019, 46(9): 0902002.
- [8] 吴雪峰, 尹海亮, 李强. 飞秒激光加工碳纳米管薄膜试验研究 [J]. 中国激光, 2019, 46(9): 0902002.
- [9] Li D Y, Nasir I, Song Y H, et al. Femtosecond laser irradiation on amorphous silicon silver thin films [J]. Chinese Journal of Lasers, 2019, 46(11): 1103002.
- [10] 李东阳, Nasir I, 宋宇浩, 等. 非晶硅银薄膜的飞秒激光辐照研究 [J]. 中国激光, 2019, 46(11): 1103002.
- [11] Bian Y C, Wang Y L, Xiao Y, et al. Controllable micro/nano structure surface fabricated by femtosecond laser and its applications [J]. Laser & Optoelectronics Progress, 2020, 57(11): 111406.
- [12] 边玉成, 王宇龙, 肖轶, 等. 飞秒激光制备可控微纳米结构表面及应用研究 [J]. 激光与光电子学进展, 2020, 57(11): 111406.
- [13] Liang R, Hu A M, Li W J, et al. Enhanced degradation of persistent pharmaceuticals found in wastewater treatment effluents using TiO<sub>2</sub> nanobelt photocatalysts [J]. Journal of Nanoparticle Research, 2013, 15(10): 1990.
- [14] Lin L C, Liu L, Musselman K, et al. Plasmonic-radiation-enhanced metal-oxide nanowire heterojunctions for controllable multilevel memory [J]. Advanced Functional Materials, 2016, 26(33): 5979-5986.
- [15] Nakajima T, Tsuchiya T, Kumagai T. Pulsed laser-induced oxygen deficiency at TiO<sub>2</sub> surface: anomalous structure and electrical transport properties [J]. Journal of Solid State Chemistry, 2009, 182(9): 2560-2565.
- [16] Lin L C, Zou G S, Liu L, et al. Plasmonic engineering of metal-oxide nanowire heterojunctions in integrated nanowire rectification units [J]. Applied Physics Letters, 2016, 108(20): 203107.
- [17] Xing S L, Lin L C, Zou G S, et al. Improving the electrical contact at a Pt/TiO<sub>2</sub> nanowire interface by selective application of focused femtosecond laser irradiation [J]. Nanotechnology, 2017, 28(40): 405302.
- [18] Maier S A. Plasmonics: fundamentals and applications [M]. New York: Springer Science & Business Media, 2007: 21-38.
- [19] Kwon D H, Kim K M, Jang J H, et al. Atomic structure of conducting nanofilaments in TiO<sub>2</sub> resistive switching memory [J]. Nature Nanotechnology, 2010, 5(2): 148-153.
- [20] Xu W T, Min S Y, Hwang H, et al. Organic core-sheath nanowire artificial synapses with femtojoule energy consumption [J]. Science Advances, 2016, 2(6): e1501326.

- [18] Arnold A J, Razavieh A, Nasr J R, et al. Mimicking neurotransmitter release in chemical synapses via hysteresis engineering in MoS<sub>2</sub> transistors [J]. ACS Nano, 2017, 11(3): 3110-3118.

## Nanowelding and Electrical Performance Tuning of Pt-TiO<sub>2</sub> Induced by Femtosecond Laser

Xing Songling, Xiao Yu, Huo Jinpeng, Lin Luchan, Shen Daozhi, Liu Lei\*

*Department of Mechanical Engineering, Tsinghua University, Beijing 100084, China*

### Abstract

**Objective** With manufacturing being downsized to the nanoscale, the welding and joining of nanoscale materials (“nanowelding” for short) has become key in the integration of advanced nanodevice fabrication and packaging. As a bottom-up process, nanowelding can flexibly combine nanostructures with different chemical compositions and selectively modify the interfaces of semiconductor heterojunctions in order to obtain complex electrical and optical properties. In recent years, although the research on nanowelding has made significant progress, the basic theory of low-damage joining of heterojunctions at the nanoscale has not been well-established. Femtosecond (fs) laser is now widely used in the precision machining of materials with high melting point or high damage threshold due to its unique “cold” processing characteristics. In particular, optical irradiation-induced surface plasmonic effect on the metal-dielectric interface can affect the energy redistribution in the nanostructures, which is beneficial for heterogeneous interface modification of semiconductors at the nanoscale. In this study, the nanowelding process of Pt electrodes and TiO<sub>2</sub> nanowires under localized fs laser irradiation has been reported. The creation of this welded structure shows good performance of the synaptic response, which indicates a new method to realize the modification of a metal-oxide heterointerface.

**Methods** Pt/Ti (the thick is 200 nm/5 nm) electrodes with special finger spacing were fabricated by optical lithography and lift-off processes on oxidized Si substrate. TiO<sub>2</sub> nanowires with pure rutile phase were synthesized by a hydrothermal process, dispersed and diluted in a high-purity acetone solution, which was then drop-cast on the chip with Pt electrodes. The fs laser beam, with 50 fs pulse duration, 800 nm wavelength, and 1 kHz frequency, was generated from a Ti:sapphire laser system and focused by an objective lens with a numerical aperture of 0.5 at a nanoscale spot overlapping a small portion of the nanowire at the junction. COMSOL Multiphysics v5.2 with a RF module was used to simulate the electric field distribution around the Pt-TiO<sub>2</sub> nanoscale structure under polarized Gaussian beam excitation. The morphology of the welded structure was examined by scanning electron microscopy (SEM) and atomic force microscopy (AFM). The electrical characteristic was measured by a precision source and s measuring unit (Agilent B2901A) in a voltage sweeping mode at room temperature.

**Results and Discussions** Under focused fs laser irradiation, the TiO<sub>2</sub> nanowire deposited on a Pt substrate exhibits a limited damaging effect. By adjusting the incident laser fluence to 5.02 mJ/cm<sup>2</sup>, the nanowelding of Pt-TiO<sub>2</sub> was obtained (Fig. 3). The mechanical strength of the welded Pt-TiO<sub>2</sub> bonding can be evaluated by “contact AFM”. The coincidence of the loading/unloading force curves, corresponding to the extend/retract process of the probe, indicates a reliable welded bonding at the irradiated location. In contrast, the separation of the loading/unloading force curves indicates that the nanowire does not remain bound to the Pt electrode without laser irradiation and moves away during the extend/retract process (Fig. 4). The bonding between the TiO<sub>2</sub> nanowire and the Pt electrode is mainly facilitated by the formation of “hotspots”, which is known to result from localized plasmonic field enhancement (Fig. 6). During the welding process, the Magnéli phase (oxygen deficient TiO<sub>2-x</sub>) is formed at the Pt-TiO<sub>2</sub> contact by redox reactions under high intensity excitation. The layer contains a high defect concentration, which is beneficial for the wettability of the Pt-TiO<sub>2</sub> interface as well as the reduction of the heterointerface barrier height. The electrical characteristics show that after fs laser welding on one side of the TiO<sub>2</sub> nanowire contacted with the two Pt electrodes, there is an obvious self-rectifying current response at a bias of -10/+10 V (Fig. 7). Besides, the introduced TiO<sub>2-x</sub> layer during nanowelding is helpful for the synaptic plasticity of the TiO<sub>2</sub> nanowire as an artificial synapse. For the initial TiO<sub>2</sub> synapses, multilevel excitatory postsynaptic current amplification is observed under voltage cycling. Unlike the unwelded units, the maximum amplified current in the welded structure is

stabilized during the first ten cycles (Fig. 10). The current accumulation and decay properties of the artificial synapse to simulate the learning/forgetting response of human memory are also investigated. The repeated application of input pulses induces an enhancement in the current response stability, which suggests the transition from short-term potentiation to long-term potentiation in the  $\text{TiO}_2$  synapse by repeated stimulation.

**Conclusions** We have demonstrated a method for welding  $\text{TiO}_2$  nanowires on Pt electrodes that utilizes plasmonic effect induced by fs laser irradiation. The welded bonding of Pt- $\text{TiO}_2$  can be obtained at a fluence of  $5.02 \text{ mJ/cm}^2$ , which has been confirmed by the “contact AFM”. Strong plasmonic-enhanced electric fields induced by tightly-focused fs laser irradiation exist at the Pt- $\text{TiO}_2$  interface and contribute to the formation of localized oxygen deficiencies (Magnéli phases). This introduced component improves the wettability of the  $\text{TiO}_2$  nanowire on the Pt electrodes and reduces the interfacial barrier height, which results in the stability of the  $\text{TiO}_2$  synapse. Based on the welded Pt- $\text{TiO}_2$  structure, the synaptic plasticity of a single  $\text{TiO}_2$  nanowire is presented, which shows potential in replicating the complicated learning/forgetting process.

**Key words** laser technique; nanowelding and nanojoining; femtosecond laser; memristor; synaptic plasticity;  $\text{TiO}_2$  nanowire

**OCIS codes** 140.3390; 320.2250; 320.708